Proceedings World Geothermal Congress 2015
Melbourne, Australia, 19-25 April 2015

3D Inversion of Magnetotelluric Data from the Sipoholon Geothermal Field, Sumatra, Indonesia

Sintia W. Niasari[1,3], Gerard Muñoz[1], Muhammad Kholid[2], Edi Suhanto[2] and Oliver Ritter[1]

[1]GFZ German Research Centre for Geosciences, Telegrafenberg, 14473 Potsdam, Germany

[2]PSDG Center for Geological Resources, Jl. Soekarno-Hatta 444, 40122 Bandung, Indonesia

[3]Geophysics Study Program, Physics Department, F. MIPA- UGM, Sekip Utara, 55281 Yogyakarta, Indonesia

sintia_windhi@yahoo.com, gmunoz@gfz-potsdam.de, kholid_di@yahoo.com, edi.suhanto@gmail.com, oritter@gfz-potsdam.de

Keywords: magnetotelluric, non-volcanic geothermal system, Sumatra, exploration, 3D inversion

ABSTRACT

The Sipoholon geothermal field has been identified as a moderate temperature geothermal system based on geothermometry. This geothermal field is characterised by 18 hot springs and located around the Tarutung basin, a pull-apart basin along the Sumatra fault. Debates continue on how this geothermal system works.

3D inversion of magnetotelluric (MT) data has been performed using the ModEM code. Six different schemes (using different components, rotation, and error floor settings) were used to investigate the effect of each scheme on the model result. Although the inversion results of the six schemes exhibit different conductivity contrasts, all of them display similar structures. All models show a shallow conductive anomaly beneath the Tarutung basin and a vertically elongated conductor at the eastern part of the Tarutung basin. The shallow conductor beneath the Tarutung basin is interpreted as unconsolidated sediments of volcanic origin, e.g. the young Toba Tuff (74 ka). The vertical conductor coincides with the location of Panabungan hot spring and normal fault zones. This vertical conductive zone indicates a circulating hot fluid heated up by deep magmatic activity due to the subduction process.

1. INTRODUCTION

Magnetotelluric (MT) measurements are used widely for geothermal exploration (e.g. Spichak and Manzella, 2009). The MT method is a passive electromagnetic method which uses electric and magnetic field variations of natural origin (Vozoff, 1990). The relation between electric and magnetic fields as a function of period (or frequency) determines the subsurface electrical conductivity distribution (Tikhonov, 1950; Cagniard, 1953).

As of 2000, three-dimensional (3D) inversions of MT data have been used for geothermal exploration (Yamane et al., 2000). The development of 3D inversion of MT data is growing vastly along with the development of computing hardware. The present work is aimed to investigate the 3D model of subsurface electric conductivity distribution of the Sipoholon geothermal filed located on densely populated regions of Sumatra, Indonesia (Figure 1).

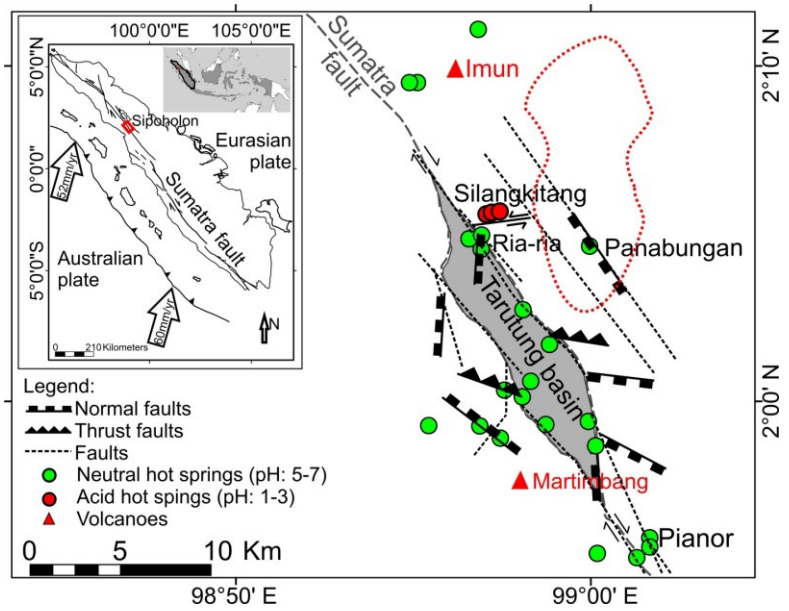

Figure 1: Location of hot springs (green circles), inactive volcanoes (red triangles), faults and the Tarutung basin. Red circles indicate the Silangkitang acidic hot springs which are close to a sealed sinistral fault. The grey area indicates the distribution of the alluvium deposit in the Tarutung basin (modified from Nukman and Moeck, 2013). Dashed red contour marks the high Vp/Vs ratio (>1.75) at 2 km depths (modified from Muksin et al., 2013). Inset: Map of Sumatra showing the subduction zone and motion of the plate (indicated by arrows) (modified from Sieh and Natawidjaja, 2000).

The Sipoholon geothermal filed is situated in the vicinity of the Sumatra Fault (Figure 1). The Sumatra Fault is a 1650 km strike slip fault due to oblique subduction between the Eurasian and Australian plates (Sieh and Natawidjaja, 2000). The subduction also resulted on magmatic activity along the Sumatra fault (Sieh and Natawidjaja, 2000).

18 hot springs are distributed inside and around the Tarutung basin, including the Panabungan (PNB) hotspring (Figure 1). The PNB hot spring is located close to a normal fault zone which is part of a negative flower structure of the Sumatra fault in this area (Nukman and Moeck, 2013). Fluid samples of the PNB show low ratio of deuterium and oxygen indicating that the water contains magmatic waters from depth mixed with surface waters (Nukman, 2014). The PNB fluid samples also exhibit neutral pH, indicating an up-flow zone of the Sipoholon geothermal field (Nukman, 2014). Additionally, a high Vp/Vs anomaly found beneath the PNB at 2 km depths interpreted as high fluid content in porous media (Muksin et al., 2013).

Here, we performed separate inversions to investigate the effects of the data components, rotation and error floor settings in the inversion model results, particularly on the structures close to the PNB. We compare horizontal sections of each model as well as cross section along a profile. Accordingly, interpretation of the structures resulted from the inversion is also discussed.

2. MAGNETOTELLURIC METHOD

2.1 Magnetotelluric Data

On July 2011, an MT survey consisting of 70 sites was conducted to investigate the subsurface of the Sipoholon geothermal field. Site spacing was approximately 1 km covering an area of (23 x 25) km^2, except at some sites due to the presence of high voltage power lines and accessibility problems. Five components (Ex, Ey, Hx, Hy, and Hz) were measured with one additional permanent remote reference (RR) site. The magnetic fields were measured using Metronix MFS06 and MF07 induction coils. Non-polarizable silver-silver chloride electrodes measured the horizontal electric fields. All sensors were connected to the sensor box which was linked to the S.P.A.M. (Short-Period Automatic Magnetotelluric) MkIV real time MT systems. The S.P.A.M. MkIV recorded data in the frequency range 0.003 Hz to 10 kHz.

The data were processed using the robust processing algorithms of the EMERALD software package (Ritter et al., 1998; Weckmann et al., 2005; Krings, 2007; Chen, 2008). The data processing consists of two steps, the single site processing and the remote reference (RR) processing steps. Delay line filtering was applied to the single site processing to improve the data quality in high frequency (>50 Hz). The RR technique was applied to improve the data quality in low frequency (< 0.1 Hz). An EDI file for each site was created from a combination of data from single site and remote reference processing.

Due to the data quality, in this 3D inversion study, we used only 51 from 70 MT sites. The phase-tensor ellipse map and real induction vectors at a period of 1 s of these 51 sites are displayed in Figure 2. Plotting the phase tensor ellipses together with the real induction arrows at certain period gives not only information about the dimensionality, but also the about the (possible) strike direction (Booker, 2013). As shown in Figure 2, the real induction arrows (Wiese convention) and the axes of the phase tensor ellipses are not always aligned. For 1-D and 2-D case, the real induction arrows and the axes of the phase tensor ellipse are expected to be collinear (Caldwell et al., 2004). For a 3-D case, the ellipse major axis and the real induction arrows are not aligned.

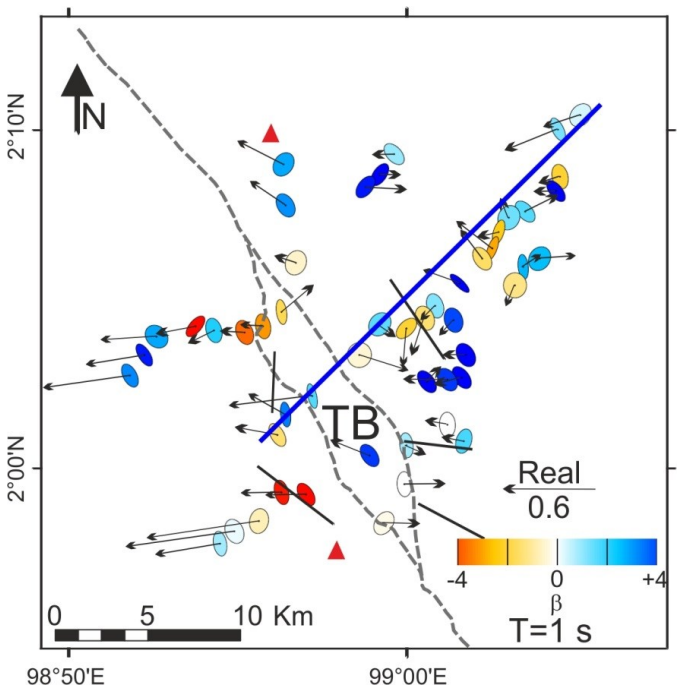

Figure 2: Observed phase tensor ellipses and real induction arrows (Wiese convention) at a period of 1 s. The ellipses are normalized with maximum principal axis. Colours filling the ellipses show the phase tensor skew angle (β). Black lines indicate surface trace of normal faults. Blue line marks a profile shown in Figure 4. Dashed grey lines mark the Sumatra fault and the Tarutung basin. Most of the sites close to the normal faults exhibit high values of β (as indicated by red or blue colours), indicating a 3-D character. Induction vectors display stronger conductivity contrast in the western part of the (TB) than in the eastern part. Most of the real induction vectors point away from the basin, e.g. to the W.

2.2 3D Inversion of MT Data

3D inverse modelling was carried out using the Mod3DEM (Egbert and Kelbert, 2012 and Meqbel, 2009). For the inversion, the data at 51 sites for a period range of 0.001-1000 s was used. The data was selected carefully, omitting noisy soundings with large scatter or large error bars. The data consist of the full impedance and the vertical magnetic transfer functions (VTFs). The grid cell dimensions were 500 x 500 m in lateral extent for the inner grid, with 10 padding cells increasing by a factor 1.5 at each direction. The vertical grid increases by factor 1.2 starting from 50 m. The total numbers of cells is 80 x 80 x 40.

We performed six different inversion schemes (see Table 1 in the following section). 3D inversion of models A and B were carried out to study the sensitivity of VTFs data, while the 3D inversion of model A-D were carried out to investigate the conductivity contrast dependency on data and grid rotation, especially beneath the PNB. Additionally, 3D inversion of models E and F were performed to analyse the sensitivity of the diagonal elements of the impedance and the VTFs.

Table 1. Six schemes of the 3D inversion used in this study, including the setting of each schemes.

Model's name	Data and grid rotation (deg)	Data components	Error floor setting	Total iteration numbers	Global RMS misfit
A	0	Full impedance	Zxx = Zyy = 5%;Zxy = Zyx = 3%	69	2.1
B	0	Full impedance and VTFs	Zxx = Zyy = 5%; Zxy = Zyx = 3%;Tzx = Tzy = 0.03	77	1.8
C	-36	Full impedance	Zxx = Zyy = 5%;Zxy = Zyx = 3%	114	2.9
D	-36	Full impedance and VTFs	Zxx = Zyy = 5%; Zxy = Zyx = 3%;Tzx = Tzy = 0.03	91	2.8
E	0	Full impedance and VTFs	Zxx = Zyy = 30%; Zxy = Zyx = 3%; Tzx = Tzy = 0.03	74	1.6
F	0	Full impedance and VTFs	Zxx = Zyy = 5%; Zxy = Zyx = 3%;Tzx = Tzy = 0.3	67	1.7

3. RESULTS

All models present similar features (Figure 3), such as a very resistive body (R1) in the south-westernmost region of the study area. The Permian granite border from surface map from Nukman and Moeck (2013) is collocated with feature R1. A shallow conductive anomaly (C1) is imaged consistently beneath the TB. The inversion result of model B shows feature C1 reach 1 Ωm at 1 km. In addition, a conductive anomaly (C2) that continues at depth (Figure 4) is located around the PNB hot spring and normal fault. Feature C2 has a resistivity below 10 Ωm in all models, but slightly different conductance. The lateral resistive discontinuity is in good correlation with a NW-SE PNB normal fault zone from surface mapping by Nukman and Moeck (2013). Beneath the inactive Martimbang volcano, a conductive body (C4) with less than 10 Ωm appears in some models (in model B, C4 is located beneath the hot springs and a normal fault) but not in others (such as A or F).

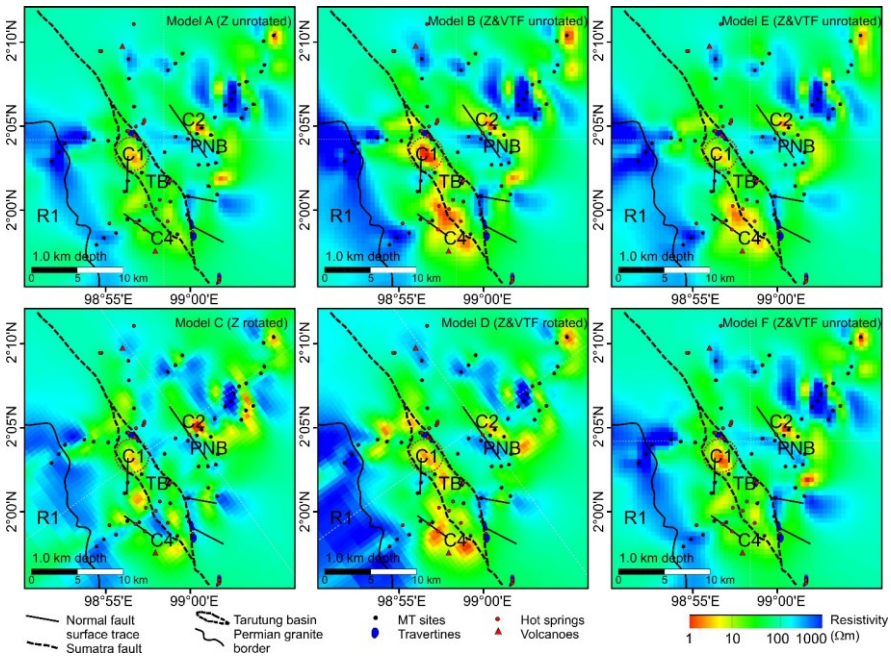

Figure 3: Resistivity in the Sipoholon area at 1.0 km depth from 3D inversions of MT data. Red dots: hot springs; black dots: MT soundings; thick black lines: Permian granite contour lines from surface mapping; dashed black lines: the Tarutung basin area. Low resistivity anomalies (< 10 Ωm) correspond to red and yellow colours, such as those appearing beneath the Tarutung basin. High resistivity anomalies (>100 Ωm) correspond to blue colours, such as those appearing beneath the Permian granite in the Western part of the study area.

The differences between each model are number of iteration needed until the model converge and total RMS misfits (see Table 1) as well as conductivity contrasts. Inversion of un-rotated impedances and VTFs (model B) exhibits the strongest conductivity contrast beneath the TB. The rotated impedances and VTFs (model D) displays less conductivity contrast compared to the un-rotated impedances and VTFs (model B). The model result using an error floor of 30 per cent of $|Zxy * Zyx|^{1/2}$ for the diagonal elements (i.e. downweighting the main diagonal elements) in model E also shows less conductivity contrast. The preferred inversion model is the inversion result of model B, using un-rotated impedance and VTFs.

Figure 4 shows the comparison between 2D and 3D inversion results of both preferred model along a profile (indicated by blue line in Figure 2). The 2D and 3D inversion approaches have some differences, such as different mesh construction. However, the 2D and 3D inversion results reveal similar conductivity structures, such as features R1 and R2. The Tarutung basin is represented as a shallow conductor (C1) with resistivity less than 10 Ωm at depth down to 2 km in both approaches. The upper part of the conductor close to PNB (C2) extends vertically down to 4 km depths in both model results. However, the lower part of this conductor is not imaged in the 3D inversion result.

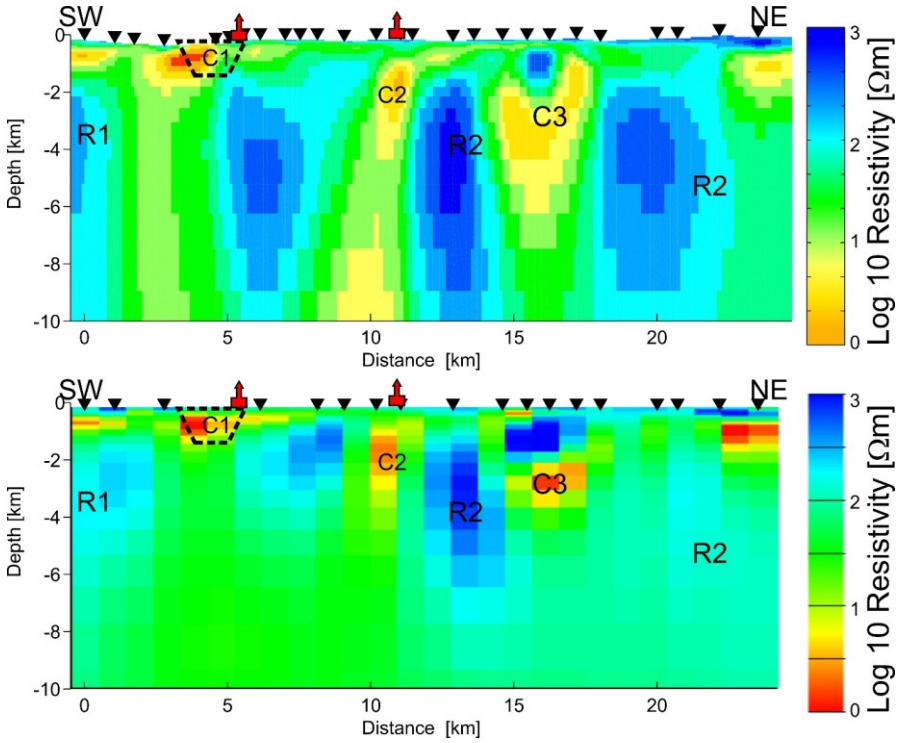

Figure 4: SW-NE resistivity sections across a profile obtained from 2D inversion (above) and 3D inversion (below). Inverted triangles: MT stations. Profile location is shown as a blue line in the Figure 2. Low resistivity anomalies (< 10 Ωm) are represented with red and yellow colours and are labelled as C. High resistivity anomalies (> 100 Ωm) are shown in blue colours and labelled as R. To clarify, the smallest cell size used in 2D and 3D inversions are different (i.e. 70 m and 500 m, respectively). Both 2D and 3D inversion results display similar structures, such as a shallow conductor beneath the Tarutung basin (marked by black dashed trapezium). However, 2D inversion resulted in deeper extension of structures than 3D inversion.

4. DISCUSSION

The resistive body R1 (see Figure 3) at the surface corresponds to the Permian granite. This Permian granite in the SW region of the study area (see Figure 3) could be impermeable so then it gives high resistivity response which means no fluid path ways and no fluid accumulation. Together with this, this impermeable granite might be the south-western border of the Sipoholon geothermal system as indicated by the absence of any geothermal manifestation, such as hot spring. The area between the Permian granite and the TB at the surface coincides with weathered Miocene andesite where the area shows a resistivity between 50-100 Ωm. In the southern part, this resistive area is interrupted by a conductive anomaly (C4) around a cluster of hot springs close to the inactive Martimbang volcano. This conductive zone occurs down to 2 km depths and might be correlated to the presence of thermal fluids. An alternative explanation of C4 is hydro-thermally altered Andesitic material due to high temperatures in the past when the intrusion of Martimbang volcano occurred.

The shallow conductor (C1), shown in red, beneath the TB is interpreted as unconsolidated sedimentary filling. This alluvium comes from the higher areas to the East and to the West of the basin. From a discontinuity in the Vp tomography model, the Tarutung basin was interpreted as having a depth of 2 km by Muksin et al. (2013). At depths, below 2 km, with resistivity values between 10 and 100 Ωm, the anomaly could be related to the Sumatra fault. This conductor separates R1 and R2 and coincides with a concentration of local earthquake between 2 km and 11 km depths beneath the Sumatran fault (Muksin et al., 2013).

Conductor C2 can be divided into two parts, the upper part down to 4 km depths and the deeper part below 8 km depths. The upper part of C2 is interpreted as a fluid path ways, both from the reservoir to the surface manifestation and from the surface to the

reservoir. This interpretation is based on structural geology finding, which interpret the PNB normal fault zone as part of a negative flower structure and therefore of a fracture system (Nukman and Moeck 2013, Nukman, 2014). The reservoir itself could be around 2 km depths where the highest conductivity occurs (see Figure 4). Unlike in volcanic geothermal systems, the reservoir zone of the Sipoholon non-volcanic geothermal system is not characterised by the electrically resistive prophylitic alteration mineral. The conductive zone is due to hot saline water accumulated at depths. The lower part of C2 could be related to fluid path ways of magmatic water which might be originated by subduction processes at depth. This hot magmatic water, as indicated from the geo-chemistry study of Nukman (2014), could be the heat source of the Sipoholon geothermal system.

5. CONCLUSION

Using the ModEM3DMT, we can control the input data, whether full impedances, VTFs or a combination of both. This has the advantage that we can analyse which components of the data control the subsurface information and which components have lower data quality. However, this is computationally expensive.

Although those six models have different data input and settings, all of them reveal similar conductivity features. This means that data and grid rotation is not necessary for 3D inversion of the Sipoholon MT data. Accordingly, the conductivity features appearing in 3D inversion are also present in 2D inversion, suggesting the robustness of these features. Our results show that the 3D inversion without rotating data and grid can be effectively used in a relatively 2D geological setting, such as in the Sipoholon area.

All inversion models image a vertical conductor, extending from surface to approximately 4 km depth, in the eastern part of the Tarutung basin. This vertical conductor coincides with the location of Panabungan hot spring and normal fault. This deep reaching conductive zone reveals possible fluid pathways, both for recharge of meteoric water and for ascending magmatic water from a possible deeper reservoir. The geothermal reservoir in-between is heated up by the circulating hot fluids, which originate from magmatic activity related to the subduction process. Our interpretation is consistent with geochemical studies which indicate magmatic origin for fluids sampled from the Panabungan hot spring.

REFERENCES

Booker, J. R.: The Magnetotelluric Phase Tensor: A Critical Review, *Surv. Geophys.*, **35**, (2013), 7-40.

Cagniard, L.: Basic Theory of the Magnetotelluric Method of Geophysical Prospecting, *Geophysics*, **18**, (1953), 605-635.

Caldwell, T. G., Bibby, H. M., and Caldwell, C.: The Magnetotelluric Phase Tensor, *Geophysical Journal International*, **158**, (2004), 457-469.

Chen, X.: Filterung von Geophysikalischen Zeitreihen mit Periodisch Auftretenden Multifrequenten Störsignalen, *Diploma Thesis*, Technischen Universität Berlin, Germany (2008).

Egbert, G. D., and Kelbert, A.: Computational Recipes for Electromagnetic Inverse Problems, *Geophysical Journal International*, **189**, (2012), 251-267.

Krings, T.: The Influence of Robust Statistics, Remote Reference, and Horizontal Magnetic Transfer Functions on Data Processing in Magnetotellurics, *Master thesis*, Universität Münster, Germany (2007).

Meqbel, N. M. M.: The electrical conductivity structure of the Dead Sea Basin derived from 2D and 3D inversion of magnetotelluric data, *PhD thesis*, Free University of Berlin (2009).

Muksin, U., Bauer, K., and Haberland, C.: Seismic Vp and Vp/Vs structure of the geothermal area around Tarutung (North Sumatra, Indonesia) derived from local earthquake tomography, *Journal of Volcanology and Geothermal Research*, **260**, (2013), 27–42.

Niasari, S. W., Muñoz, G., Kholid, M., and Ritter, O.: 2D electrical conductivity image of the Sipoholon geothermal system, Sumatra, Indonesia, submitted in *Geothermics*.

Nukman, M.: Geothermal Exploration Involving Structural Geology and Hydro-chemistry in the Tarutung Basin, Northern Central Sumatra (Indonesia), *Phd thesis*, Fakultät VI, Technischen Universität Berlin, Germany (2014).

Nukman, M., and Moeck, I.: Structural Controls on a Geothermal System in the Tarutung Basin, North Central Sumatra, *Journal of Asian Earth Sciences*, **74**, (2013), 86-96.

Ritter, O., Junge, A., and Dawes, G.: New Equipment and Processing for Magnetotelluric Remote Reference Observations, *Geophysical Journal International*, **132**, (1998), 535-548.

Sieh, K., and Natawidjaja, D.: Neotectonics of the Sumatra Fault, Indonesia, *Journal of Geophysical Research*, **105**, (2000), 28.295-28.326.

Spichak, V., and Manzella, A.: Electromagnetic sounding of geothermal zones, Journal of Applied Geophysics, 68, (2009), 459–478.Tikhonov, A. N.: On Determining Electrical Characteristics of the deep layers of the Earth's crust, *Dok. Akad. Nauk., USSR*, **73**, (1950), 295-297.

Vozoff, K.: Magnetotellurics: Principles and practice, Earth Planet. Sci., 99, (1990), 441-471.Weckmann, U., Magunia, A., and Ritter, O.: Effective Noise Separation for Magnetotelluric Single Site Data Processing Using a Frequency Domain Selection Scheme, *Geophysical Journal International*, **161**, (2005), 635-652.

Yamane, K., Ohsato, K., Ohminato, T., and Kim, H. J.: Three-Dimensional Magnetotelluric Investigation in Kakkonda Geothermal Area, Japan, Proceedings, World Geothermal Congress, Kyushu-Tohoku, Japan (2000).